Implementation and Assessment of a Simple Nonlocal van der Waals Density Functional

Oleg A. Vydrov and Troy Van Voorhis

Department of Chemistry, Massachusetts Institute of Technology, Cambridge, MA, 02139, USA

(Dated: 9 April 2010)

Recently we developed a nonlocal van der Waals density functional (VV09) that has a simple and well-behaved analytic form. In this article, we report a self-consistent implementation of VV09 with an atom-centered basis set. We compute binding energies for a diverse benchmark set and find that VV09 performs well in combination with Hartree-Fock exchange. We compare VV09 with its precursor, discuss likely sources of inaccuracies in both models, and identify some aspects of the methodology where further refinements are desirable.

I. INTRODUCTION

Applications of the Kohn–Sham density functional theory (DFT)[1] rely on approximations to the exchange-correlation (xc) energy.[2] Local and semilocal xc functionals dominate computational materials science. For molecules, the most successful and popular xc models are the so-called 'hybrids', where a fraction of exact (Hartree–Fock-like) exchange is admixed to a semilocal xc functional.[2] Despite the impressive performance for many physical and chemical properties of molecules and dense materials, common xc functionals share some well-known deficiencies, such as inability to properly describe dispersion interactions.[3] Long-range correlation effects that give rise to van der Waals attraction cannot in principle be captured by semilocal correlation functionals. Reliable treatment of dispersion interactions requires fully nonlocal correlation models. Nonlocality can be introduced via explicit dependence on Kohn–Sham orbitals (both occupied and virtual), as exemplified by the random phase approximation (RPA) and related methods.[4–9] Recently, it has been demonstrated that it is possible to describe the entire range of van der Waals interactions in a general and seamless fashion by a nonlocal correlation functional that depends only on the electron density and includes no explicit orbital dependence.[10–12] Van der Waals functionals of Refs. 10–12 allow for a self-consistent treatment[13–16] of dispersion interactions. By contrast, practical applications of RPA methods[4–9] or force-field-like dispersion corrections[17–20] are typically performed in a post-self-consistent fashion, using electron densities produced by a semilocal or a hybrid functional. Empirical dispersion-corrected atom-centered pseudopotentials[21,22] produce some changes in electron densities, but it is unclear whether these changes have the correct physical origin. Unlike most dispersion-corrected DFT techniques, RPA methods[4–9] and nonlocal van der Waals functionals[10–12] are truly seamless: they require neither splitting the system into interacting fragments nor any kind of atomic partitioning. The nonlocal van der Waals density functional of Ref. 12, denoted VV09, has a particularly simple analytic form. In this article we explain how VV09 is implemented self-consistently with a Gaussian basis set and show how the forces on nuclei are computed. We assess the performance of VV09 in combination with several exchange functionals on a diverse test set. For the sake of comparison, we also present the results obtained with another nonlocal van der Waals density functional, vdW-DF-04 of Ref. 10, for the same test set.

II. IMPLEMENTATION

Both vdW-DF-04 and VV09 were implemented self-consistently into the Q-Chem software package.[23] Our implementation of vdW-DF-04 was reported in Ref. 14. One important improvement has been made since Ref. 14 was published: our code can now use different numerical quadrature grids for the (semi)local and nonlocal parts of the xc functional. This enables us to use a coarser grid for evaluating the nonlocal correlation component, thus drastically reducing the computational cost without an appreciable loss in accuracy. Below we describe our implementation of VV09.

Using atomic units ($\hbar = e = m = 1$), we rewrite $E_{\rm c}^{\rm nl}$ in a different (as compared to Ref. 12) form that is more convenient for self-consistent implementation:

$$E_{\rm c}^{\rm nl} = \frac{1}{2}\int {\rm d}\mathbf{r}\, W(\mathbf{r}) \int {\rm d}\mathbf{r}'\, W(\mathbf{r}') \frac{\mathcal{D}(K) Q^6}{\omega_0(\mathbf{r}) + \omega_0(\mathbf{r}')}, \tag{1}$$

with $W = n/\omega_0$, where n is the total electron density and $\omega_0 = \sqrt{\omega_p^2/3 + \omega_g^2}$. In the latter expression we used the local plasma frequency, given by $\omega_p^2 = 4\pi n$, and the local band gap, defined as $\omega_g^2 = C|\nabla n/n|^4$, with $C = 0.0089$. Other quantities in Eq. (1) are $K = |\mathbf{r} - \mathbf{r}'| Q(\mathbf{r}, \mathbf{r}')$ and

$$Q = \frac{1}{2}\left[\frac{\kappa(\mathbf{r})\kappa(\mathbf{r}')}{\kappa(\mathbf{r}) + \kappa(\mathbf{r}')}\right]^{1/2}, \tag{2}$$

where $\kappa = 4(3n/\pi)^{1/3}\phi^2$, with the spin-scaling factor $\phi(\zeta) = [(1+\zeta)^{2/3} + (1-\zeta)^{2/3}]/2$ for the relative spin polarization $\zeta = (n_\alpha - n_\beta)/n$. The function $\mathcal{D}(K)$ in Eq. (1) is defined as

$$\mathcal{D} = \mathcal{B}\Big(2\mathcal{A} - \frac{3}{2}\mathcal{B}\Big), \tag{3}$$

$$\text{with} \quad \mathcal{A} = \frac{2}{\sqrt{\pi}}\, e^{-K^2}, \quad \text{and} \quad \mathcal{B} = \frac{\mathrm{erf}(K)}{K^3} - \frac{\mathcal{A}}{K^2}.$$

For small K, $\mathcal{B}$ can be replaced by its truncated Taylor series expansion. For large K, $\mathcal{D}(K) \to -3/(2K^6)$ and thus $\mathcal{D}(K)Q^6 \to -3/(2|\mathbf{r} - \mathbf{r}'|^6)$. Note that $\mathcal{D}(K)$ of Eq. (3) is different from $D(K)$ used in Ref. 12, hence the different typeface.

In terms of an atom-centered basis set $\{\chi_\mu(\mathbf{r})\}$, the electron spin-density is expressed as

$$n_\sigma(\mathbf{r}) = \sum_{\mu\nu} P_{\mu\nu}^\sigma\, \chi_\mu(\mathbf{r})\chi_\nu(\mathbf{r}), \tag{4}$$

where $P_{\mu\nu}^\sigma$ are the density matrix elements and $\sigma \in \{\alpha, \beta\}$ labels the spin. For a self-consistent implementation, we need to find the derivatives of $E_{\rm c}^{\rm nl}$ with respect to $P_{\mu\nu}^\sigma$:

$$\frac{{\rm d}E_{\rm c}^{\rm nl}}{{\rm d}P_{\mu\nu}^\sigma} = \int {\rm d}\mathbf{r}\, \chi_\mu(\mathbf{r}) \frac{\delta E_{\rm c}^{\rm nl}}{\delta n_\sigma(\mathbf{r})} \chi_\nu(\mathbf{r}). \tag{5}$$

To that end, we employ the standard formalism[24] developed for semilocal xc functionals:

$$\frac{\mathrm{d}E_{\mathrm{c}}^{\mathrm{nl}}}{\mathrm{d}P_{\mu\nu}^{\sigma}} = \int \mathrm{d}\mathbf{r}\Big[F_n^{\sigma}\chi_\mu\chi_\nu + 2F_\gamma \nabla n\cdot\nabla\big(\chi_\mu\chi_\nu\big)\Big]. \tag{6}$$

The variable $\gamma = |\nabla n|^2$ is used for convenience of implementation. Note that $E_{\mathrm{c}}^{\mathrm{nl}}$ depends only on ∇n, but not on ∇n_α and ∇n_β. F_n^σ and F_γ in Eq. (6) are computed as

$$F_\gamma(\mathbf{r}) = -\frac{\partial\omega_0}{\partial\gamma}(\mathbf{r})W(\mathbf{r})\left[\frac{1}{\omega_0(\mathbf{r})}\int \mathrm{d}\mathbf{r}'\,U(\mathbf{r},\mathbf{r}')\mathcal{D}(K) + \int \mathrm{d}\mathbf{r}'\frac{U(\mathbf{r},\mathbf{r}')\mathcal{D}(K)}{\omega_0(\mathbf{r})+\omega_0(\mathbf{r}')}\right], \tag{7}$$

and

$$\begin{aligned} F_n^\sigma(\mathbf{r}) = {}& \frac{1}{\omega_0(\mathbf{r})}\Big[1 - \frac{\partial\omega_0}{\partial n}(\mathbf{r})W(\mathbf{r})\Big]\int \mathrm{d}\mathbf{r}'\,U(\mathbf{r},\mathbf{r}')\mathcal{D}(K) \\ & - \frac{\partial\omega_0}{\partial n}(\mathbf{r})W(\mathbf{r})\int \mathrm{d}\mathbf{r}'\frac{U(\mathbf{r},\mathbf{r}')\mathcal{D}(K)}{\omega_0(\mathbf{r})+\omega_0(\mathbf{r}')} \\ & + \frac{\partial\kappa}{\partial n_\sigma}(\mathbf{r})\frac{W(\mathbf{r})}{\kappa^2(\mathbf{r})}\int \mathrm{d}\mathbf{r}'\,U(\mathbf{r},\mathbf{r}')\mathcal{G}(K)Q^2. \end{aligned} \tag{8}$$

In Eqs. (7) and (8) we introduced two new quantities:

$$U(\mathbf{r},\mathbf{r}') = \frac{W(\mathbf{r}')Q^6}{\omega_0(\mathbf{r})+\omega_0(\mathbf{r}')}, \tag{9}$$

and

$$\mathcal{G} = 8\mathcal{A}\big(\mathcal{A} - K^2\mathcal{B}\big). \tag{10}$$

To within the numerical precision, $\mathcal{G} = 0$ for $K > 5$.

Within a Gaussian basis set implementation, the gradient of $E_{\mathrm{c}}^{\mathrm{nl}}$ with respect to nuclear displacements has three contributions:

$$\nabla_A E_{\mathrm{c}}^{\mathrm{nl}} = \mathbf{g}_{\mathrm{GBF}}^A + \mathbf{g}_{\mathrm{weights}}^A + \mathbf{g}_{\mathrm{grid}}^A. \tag{11}$$

$\mathbf{g}_{\mathrm{GBF}}^A$ refers to the contribution of the Gaussian basis functions. This term can be evaluated by plugging F_n^σ and F_γ into Eq. (9) of Ref. 24 instead of $\partial f/\partial n_\sigma$ and $\partial f/\partial\gamma$.

The last two terms in Eq. (11) are due to the specifics of our numerical quadrature integration technique. We use the atomic partitioning scheme developed by Becke,[25] which separates the molecular integral into atomic contributions:

$$E_{\mathrm{c}}^{\mathrm{nl}} = \frac{1}{2}\sum_A\sum_{i\in A} w_{Ai}W(\mathbf{r}_{Ai})\sum_B\sum_{j\in B} w_{Bj}U(\mathbf{r}_{Ai},\mathbf{r}_{Bj})\mathcal{D}(K), \tag{12}$$

where w_{Ai} and w_{Bj} are the quadrature weights, and the grid points $\mathbf{r}_{Ai}$ are given by $\mathbf{r}_{Ai} = \mathbf{R}_A + \mathbf{r}_i$, where $\mathbf{R}_A$ is the position of nucleus A, with the $\mathbf{r}_i$ defining a one-center integration

grid. The quadrature weights depend on the nuclear configuration and hence have a nonzero gradient with respect to nuclear displacements:

$$\mathbf{g}^A_{\text{weights}} = \sum_B \sum_{i\in B} \big[\nabla_A w_{Bi}\big] W(\mathbf{r}_{Bi}) \sum_C \sum_{j\in C} w_{Cj} U(\mathbf{r}_{Bi}, \mathbf{r}_{Cj}) \mathcal{D}(K). \tag{13}$$

The weight derivatives $\nabla_A w_{Bi}$ can be found in Ref. 24.

The last term in Eq. (11) arises because each one-center quadrature grid moves together with its parent nucleus and $\mathcal{D}(K)$ in Eq. (1) depends explicitly on the distance between the grid points $r_{ij} = |\mathbf{r}_{Ai} - \mathbf{r}_{Bj}|$. The $\mathbf{g}^A_{\text{grid}}$ term can be computed as:

$$\mathbf{g}^A_{\text{grid}} = \sum_{i\in A} w_{Ai} W(\mathbf{r}_{Ai}) \sum_{B\neq A} \sum_{j\in B} w_{Bj} U(\mathbf{r}_{Ai}, \mathbf{r}_{Bj}) Q^2 \mathcal{H}(K) \big(\mathbf{r}_{Ai} - \mathbf{r}_{Bj}\big), \tag{14}$$

where

$$\mathcal{H} = \frac{\mathcal{G} - 12\mathcal{D}}{2K^2}. \tag{15}$$

In Eq. (14), $\mathcal{H}$ and Q are implied to depend on both $\mathbf{r}_{Ai}$ and $\mathbf{r}_{Bj}$. For small K, $\mathcal{H}$ can be replaced by its truncated Taylor series expansion. For large K, $\mathcal{H}(K)Q^8 \to 9|\mathbf{r} - \mathbf{r}'|^{-8}$.

Availability of analytic forces enables us to perform structural optimizations efficiently. We reported a few geometry optimization results in Ref. 12.

III. COMPUTATIONAL DETAILS

In VV09 as well as in vdW-DF-04, the total correlation energy is defined as $E_{\text{c}}^{\text{LDA}} + E_{\text{c}}^{\text{nl}}$, where LDA denotes the local density approximation of the correlation energy, for which we use the parameterization of Perdew and Wang.[26] There is some freedom in the choice of the exchange component. However, those exchange functionals that predict binding in van der Waals complexes are obviously unsuitable. vdW-DF-04 has been used predominantly with revPBE exchange,[27] although other choices of exchange components have recently been explored.[28] The Perdew–Wang 86 (PW86) exchange functional[29] has been shown to describe the repulsive parts of van der Waals potentials rather well,[30,31] and a refit version of PW86 was recently proposed.[31] We denote this 'refit PW86' simply as rPW86 here.

Unless otherwise noted, all reported calculations were performed self-consistently with the aug-cc-pVTZ basis set. All interaction energies are counterpoise-corrected. We use the unpruned Euler–Maclaurin–Lebedev (75,302) quadrature grid to evaluate $E_{\text{c}}^{\text{LDA}}$ and

semilocal exchange, but we use a coarser SG-1 grid[32] for E_c^{nl}. This is well-justified because E_c^{nl} is much less sensitive to the fineness of the grid as compared to (semi)local functionals. For the S22 test set, we use the geometries from Ref. 33 and the recently updated reference values of binding energies from Ref. 34. The deviations of the computed binding energies from the reference values[34] are analyzed with the help of mean errors (ME), mean absolute errors (MAE), and mean absolute percentage errors (MAPE). In all tables, binding energies are reported as positive values. Hence a negative ME indicates underbinding while a positive ME means overbinding. For the interaction energy curves of the methane dimer and the benzene–methane complex, we use the same monomer geometries as in Ref. 35.

IV. TEST RESULTS

A. The S22 benchmark set

Binding energies for the S22 test set, computed with vdW-DF-04 and VV09 at the geometries of Ref. 33, are given in Table I. We tested vdW-DF-04 in combination with three different exchange models — Hartree-Fock (HF), revPBE, and rPW86. VV09 was paired with either HF or rPW86. The error statistics are summarized in Table II. Our revPBE-vdW-DF-04 results are in good agreement with the ones reported in Ref. 28 for the same test set. A number of other exchange functionals were tested in Ref. 28 for their suitability to be paired with vdW-DF-04. Although revPBE is not the best performer in this regard,[28] it has become the standard choice.[36]

For all the subsets in the S22 set, the largest errors by far are given by HF-vdW-DF-04. This is consistent with previous observations that vdW-DF-04 is incompatible with exact exchange.[14,37] VV09 performs much better with HF exchange. In fact, as Table II shows, HF-VV09 gives the smallest overall mean error for the entire S22 set among the tested methods.

As the error statistics in Table II shows, HF-VV09 tends to overbind, while rPW86-VV09 tends to underbind. vdW-DF-04 overbinds all the systems in the S22 test set when paired with HF or rPW86 exchange, but underbinds on average when paired with revPBE.

The subset of eight complexes with predominant dispersion contribution in Tables I and II provides the most relevant benchmark, since vdW-DF-04 and VV09 are presented as van

TABLE I. Counterpoise-corrected binding energies (in kcal/mol) for the S22 test set computed using two van der Waals functionals combined with several exchange approximations. All calculations were performed self-consistently with the aug-cc-pVTZ basis set. Molecular structures are from Ref. 33 and reference binding energies are from Ref. 34.

		vdW-DF-04 with			VV09 with	
Complex (symmetry)	Ref.	HF	revPBE	rPW86	HF	rPW86
Complexes with predominant dispersion contribution (8)						
CH_4 dimer (D_{3d})	0.53	1.19	0.80	1.19	0.55	0.46
C_2H_4 dimer (D_{2d})	1.50	2.92	1.20	2.45	1.31	0.72
Benzene–CH_4 (C_3)	1.45	3.04	1.43	2.59	1.53	1.00
Benzene dimer (C_{2h})[a]	2.62	5.42	2.09	4.80	3.52	2.73
Pyrazine dimer (C_s)	4.20	7.23	3.13	6.10	5.10	3.74
Uracil dimer (C_2)[b]	9.74	15.70	8.51	12.76	13.02	9.68
Indole–Benzene (C_1)[b]	4.59	8.16	3.08	6.95	6.11	4.66
Adenine–Thymine (C_1)[b]	11.66	18.74	8.67	14.59	15.90	11.33
Mixed complexes (7)						
C_2H_4–C_2H_2 (C_{2v})	1.51	2.38	1.49	2.10	1.60	1.25
Benzene–H_2O (C_s)	3.29	4.91	2.59	3.89	3.44	2.24
Benzene–NH_3 (C_s)	2.32	3.79	1.91	3.12	2.40	1.58
Benzene–HCN (C_s)	4.55	7.14	3.37	4.83	5.22	2.85
Benzene dimer (C_{2v})[c]	2.71	4.75	2.04	3.71	3.17	2.01
Indole–Benzene (C_1)[c]	5.62	8.32	4.21	6.42	6.25	4.16
Phenol dimer (C_1)	7.09	9.80	5.23	8.07	7.69	5.66
Hydrogen bonded complexes (7)						
NH_3 dimer (C_{2h})	3.17	3.84	2.42	3.63	2.65	2.29
H_2O dimer (C_s)	5.02	6.08	3.97	5.44	4.84	3.98
Formic acid dimer (C_{2h})	18.80	24.09	15.28	18.85	20.71	14.99
Formamide dimer (C_{2h})	16.12	19.87	12.95	16.30	17.01	13.09
Uracil dimer (C_{2h})[d]	20.69	25.26	17.44	20.95	22.43	17.77
2-Pyridoxine–2-Aminopyridine (C_1)	17.00	19.83	14.35	17.67	17.08	14.58
Adenine–Thymine WC (C_1)[d]	16.74	19.96	13.62	17.18	17.28	14.13

[a] 'Parallel-displaced' configuration.

[b] Stacked configuration.

[c] T-shaped configuration.

[d] Planar configuration.

der Waals density functionals. For this subset, rPW86-VV09 yields the lowest mean errors. vdW-DF-04 gives unacceptably large errors (MAPE higher than 60%) for this subset if used with HF or rPW86. At equilibrium intermonomer separations (sampled by the S22 set), revPBE exchange is on average more repulsive than HF or rPW86. For that reason, revPBE is a fairly good match for vdW-DF-04, as far as dispersion-bound systems are concerned.

TABLE II. Summary of deviations from the reference values of the binding energies reported in Table I. ME and MAE are in kcal/mol, MAPE is in percents.

	vdW-DF-04 with			VV09 with	
	HF	revPBE	rPW86	HF	rPW86
Complexes with predominant dispersion contribution (8)					
ME	3.26	−0.92	1.89	1.34	−0.25
MAE	3.26	0.99	1.89	1.39	0.29
MAPE	88.5	23.5	62.9	22.6	14.6
Mixed complexes (7)					
ME	2.00	−0.89	0.72	0.38	−1.05
MAE	2.00	0.89	0.72	0.38	1.05
MAPE	55.6	20.3	23.3	9.3	27.2
Hydrogen bonded complexes (7)					
ME	3.06	−2.50	0.35	0.64	−2.39
MAE	3.06	2.50	0.35	0.84	2.39
MAPE	21.7	19.0	4.6	6.8	18.8
Total (22)					
ME	2.80	−1.41	1.03	0.81	−1.18
MAE	2.80	1.44	1.03	0.89	1.20
MAPE	56.7	21.1	31.8	13.4	20.0

For molecular complexes bound exclusively by van der Waals interactions, HF exchange should provide an adequate representation of the repulsive wall ('Pauli repulsion'). Interaction energies should therefore be reasonably well represented by the combination of Hartree-Fock with a dispersion energy model. As we pointed out above, HF-vdW-DF-04 severely overestimates binding energies. Although HF-VV09 is a big improvement, it still tends to overbind van der Waals complexes. These observations call for an explanation. The total correlation energy in both models is expressed as $E_c^{\rm LDA} + E_c^{\rm nl}$. Could the inclusion of $E_c^{\rm LDA}$ be the reason for overbinding? In Table III we show the results for the subset of eight dispersion-bound complexes obtained using HF paired with $E_c^{\rm nl}$ and omitting $E_c^{\rm LDA}$. We see

TABLE III. Binding energies (in kcal/mol) for the dispersion-bound subset of the S22 set computed using Hartree-Fock paired with nonlocal parts of two van der Waals functionals. LDA contributions were subtracted from the values given in Table I, keeping the electron densities unchanged.

Complex (symmetry)	Ref.	HF-vdW-DF(nl)	HF-VV09(nl)
CH_4 dimer (D_{3d})	0.53	1.04	0.36
C_2H_4 dimer (D_{2d})	1.50	2.37	0.70
Benzene–CH_4 (C_3)	1.45	2.50	0.93
Benzene dimer (C_{2h})	2.62	4.15	2.14
Pyrazine dimer (C_s)	4.20	5.75	3.50
Uracil dimer (C_2)	9.74	13.89	11.09
Indole–Benzene (C_1)	4.59	6.40	4.24
Adenine–Thymine (C_1)	11.66	16.16	13.21
	ME	2.00	−0.01
	MAE	2.00	0.74
	MAPE (%)	55.3	23.8

that removal of LDA correlation significantly decreases binding energies. In other words, E_c^{LDA} contributes a sizable portion of attractive interactions at equilibrium intermonomer separations. As Table III shows, even with LDA contributions excluded, HF-vdW-DF-04 still strongly overbinds in every case. This indicates that the nonlocal vdW-DF-04 functional overestimates dispersion interactions at equilibrium distances. By contrast, Table III shows that removing E_c^{LDA} from HF-VV09 reduces MAE by the factor of two and brings ME close to zero.

B. Interaction energy curves

The binding energies for the S22 set, reported above, were computed at the accurate equilibrium geometries[33] of the complexes to facilitate direct comparisons to other benchmark calculations in the literature, performed at the same geometries. For two systems in the S22 set — the methane dimer and the benzene–methane complex — we also computed the interaction energies for a range of intermonomer separations and compared these interaction

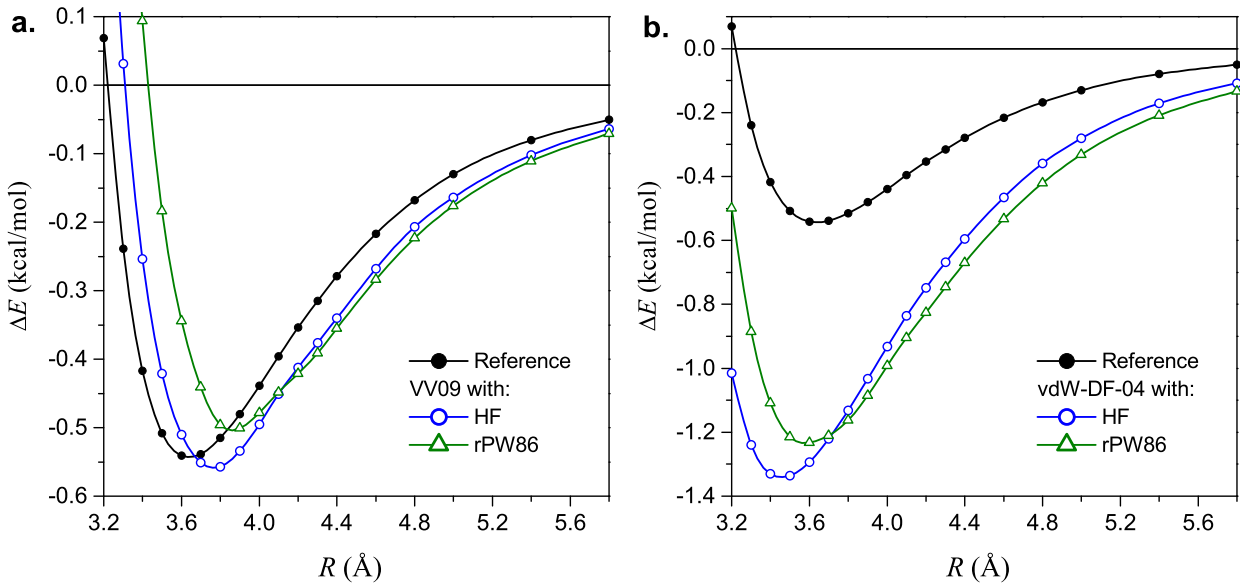

FIG. 1. Interaction energy curves for the methane dimer. R denotes the C–C distance. Accurate results from Ref. 35 compared to (a) VV09 and (b) vdW-DF-04 with two different exchange models.

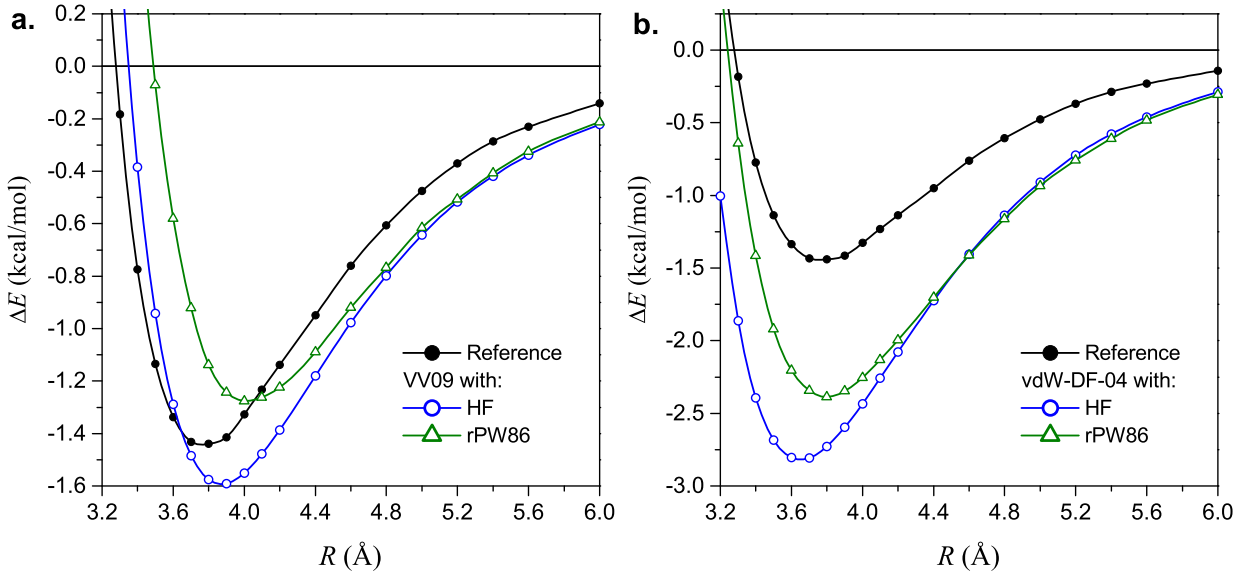

FIG. 2. Interaction energy curves for the benzene–methane complex. R is the distance between the centers of mass of the monomers. Accurate results from Ref. 35 compared to (a) VV09 and (b) vdW-DF-04 with two different exchange models.

energy curves to the accurate reference data from Ref. 35. We used the same fixed monomer geometries as in Ref. 35 and applied counterpoise corrections at every point.

For the methane dimer (Fig. 1) as well as for the benzene–methane complex (Fig. 2), both HF-VV09 and rPW86-VV09 give reasonable well-depth energies (D_e) but somewhat overestimated equilibrium intermonomer separations. vdW-DF-04 strongly overbinds both of these systems at all separations whether used with HF or with rPW86. The interaction energy curve for the benzene–methane complex computed with revPBE-vdW-DF-04 can be found in Ref. 38.

When the separation R is so large that the density overlap is negligible, the contribution of E_c^{LDA} is very small and nearly all of the interaction energy is due to E_c^{nl}. As Figures 1 and 2 show, both VV09 and vdW-DF-04 overestimate the interaction strength at large R in both of the systems, but the overestimation is more severe in vdW-DF-04. For instance, in the methane dimer at $R = 5.8$ Å, the accurate[35] binding energy is 0.050 kcal/mol, HF-VV09 gives 0.064, while HF-vdW-DF-04 yields 0.109 kcal/mol.

V. CONCLUSIONS

The nonlocal van der Waals functional VV09 has been implemented self-consistently and benchmarked, in comparison to vdW-DF-04, on the popular S22 test set of weakly bound complexes. Using several exchange models, we computed the binding energies for the S22 set at the reference geometries[33] and also calculated full interaction energy curves for two complexes. We find that VV09 performs reasonably well with HF exchange: among the methods considered in this study, HF-VV09 yields the smallest overall mean error for the entire S22 set. For the subset of dispersion-bound complexes, rPW86-VV09 is the best-performing combination. We confirm that vdW-DF-04 is incompatible with HF exchange: this combination severely overestimates the interaction energies for all the systems considered in this study. The standard choice of pairing vdW-DF-04 with revPBE yields more reasonable accuracy. As shown in Ref. 28, the performance can be further improved by tailoring an exchange functional specially fitted to be used alongside vdW-DF-04. In this work, we tested only pre-existing exchange functionals that were not adjusted for our specific purpose.

Fine-tuning the exchange component may not resolve all the imperfections of our methodology. The correlation energy functional itself may require further refinement. In the development of nonlocal van der Waals functionals, insufficient attention has been paid to the

balance of attractive contributions from the local and nonlocal correlation components at short range. The requirement that E_c^{nl} vanish in the uniform density limit prevents double counting, but does not guarantee good performance when E_c^{nl} is paired with E_c^{LDA}. LDA correlation contributes significantly to binding energies of van der Waals complexes. At present, it is not clear whether (and to what degree) these contributions are valid or spurious.

ACKNOWLEDGMENTS

This work was supported by an NSF CAREER grant No. CHE-0547877 and a Packard Fellowship.

REFERENCES

[1] *A Primer in Density Functional Theory*, edited by C. Fiolhais, F. Nogueira, and M. Marques (Springer, Berlin, 2003).

[2] G. E. Scuseria and V. N. Staroverov, in *Theory and Applications of Computational Chemistry: The First Forty Years*, edited by C. E. Dykstra, G. Frenking, K. S. Kim, and G. E. Scuseria (Elsevier, Amsterdam, 2005).

[3] I. C. Gerber and J. G. Ángyán, J. Chem. Phys. **126**, 044103 (2007), and references therein.

[4] F. Furche, J. Chem. Phys. **129**, 114105 (2008).

[5] J. Harl and G. Kresse, Phys. Rev. B **77**, 045136 (2008); Phys. Rev. Lett. **103**, 056401 (2009).

[6] J. Toulouse, I. C. Gerber, G. Jansen, A. Savin, and J. G. Ángyán, Phys. Rev. Lett. **102**, 096404 (2009).

[7] B. G. Janesko, T. M. Henderson, and G. E. Scuseria, J. Chem. Phys. **131**, 034110 (2009).

[8] D. Lu, Y. Li, D. Rocca, and G. Galli, Phys. Rev. Lett. **102**, 206411 (2009).

[9] H.-V. Nguyen and G. Galli, J. Chem. Phys. **132**, 044109 (2010).

[10] M. Dion, H. Rydberg, E. Schröder, D. C. Langreth, and B. I. Lundqvist, Phys. Rev. Lett. **92**, 246401 (2004); **95**, 109902(E) (2005).

[11] O. A. Vydrov and T. Van Voorhis, J. Chem. Phys. **130**, 104105 (2009).

[12] O. A. Vydrov and T. Van Voorhis, Phys. Rev. Lett. **103**, 063004 (2009).

[13]T. Thonhauser, V. R. Cooper, S. Li, A. Puzder, P. Hyldgaard, and D. C. Langreth, Phys. Rev. B **76**, 125112 (2007).

[14]O. A. Vydrov, Q. Wu, and T. Van Voorhis, J. Chem. Phys. **129**, 014106 (2008).

[15]A. Gulans, M. J. Puska, and R. M. Nieminen, Phys. Rev. B **79**, 201105 (2009).

[16]G. Román-Pérez and J. M. Soler, Phys. Rev. Lett. **103**, 096102 (2009).

[17]E. R. Johnson and A. D. Becke, J. Chem. Phys. **124**, 174104 (2006).

[18]S. Grimme, J. Comput. Chem. **27**, 1787 (2006).

[19]P. Jurečka, J. Černý, P. Hobza, and D. R. Salahub, J. Comput. Chem. **28**, 555 (2007).

[20]T. Sato and H. Nakai, J. Chem. Phys. **131**, 224104 (2009).

[21]O. A. von Lilienfeld, I. Tavernelli, U. Rothlisberger, and D. Sebastiani, Phys. Rev. Lett. **93**, 153004 (2004).

[22]I.-C. Lin, M. D. Coutinho-Neto, C. Felsenheimer, O. A. von Lilienfeld, I. Tavernelli, and U. Rothlisberger, Phys. Rev. B **75**, 205131 (2007).

[23]Y. Shao, L. Fusti-Molnar, Y. Jung, J. Kussmann, C. Ochsenfeld, S. T. Brown, A. T. B. Gilbert, L. V. Slipchenko, S. V. Levchenko, D. P. O'Neill, R. A. DiStasio Jr., R. C. Lochan, T. Wang, G. J. O. Beran, N. A. Besley, J. M. Herbert, C. Y. Lin, T. Van Voorhis, S. H. Chien, A. Sodt, R. P. Steele, V. A. Rassolov, P. E. Maslen, P. P. Korambath, R. D. Adamson, B. Austin, J. Baker, E. F. C. Byrd, H. Dachsel, R. J. Doerksen, A. Dreuw, B. D. Dunietz, A. D. Dutoi, T. R. Furlani, S. R. Gwaltney, A. Heyden, S. Hirata, C.-P. Hsu, G. Kedziora, R. Z. Khalliulin, P. Klunzinger, A. M. Lee, M. S. Lee, W. Liang, I. Lotan, N. Nair, B. Peters, E. I. Proynov, P. A. Pieniazek, Y. M. Rhee, J. Ritchie, E. Rosta, C. D. Sherrill, A. C. Simmonett, J. E. Subotnik, H. L. Woodcock III, W. Zhang, A. T. Bell, A. K. Chakraborty, D. M. Chipman, F. J. Keil, A. Warshel, W. J. Hehre, H. F. Schaefer III, J. Kong, A. I. Krylov, P. M. W. Gill, and M. Head-Gordon, Phys. Chem. Chem. Phys. **8**, 3172 (2006).

[24]B. G. Johnson, P. M. W. Gill, and J. A. Pople, J. Chem. Phys. **98**, 5612 (1993).

[25]A. D. Becke, J. Chem. Phys. **88**, 2547 (1988).

[26]J. P. Perdew and Y. Wang, Phys. Rev. B **45**, 13244 (1992).

[27]Y. Zhang and W. Yang, Phys. Rev. Lett. **80**, 890 (1998).

[28]J. Klimeš, D. R. Bowler, and A. Michaelides, J. Phys.: Condens. Matter **22**, 022201 (2010).

[29]J. P. Perdew and Y. Wang, Phys. Rev. B **33**, 8800 (1986).

[30]F. O. Kannemann and A. D. Becke, J. Chem. Theory Comput. **5**, 719 (2009).

[31]É. D. Murray, K. Lee, and D. C. Langreth, J. Chem. Theory Comput. **5**, 2754 (2009).

[32]P. M. W. Gill, B. G. Johnson, and J. A. Pople, Chem. Phys. Lett. **209**, 506 (1993).

[33]P. Jurečka, J. Šponer, J. Černý, and P. Hobza, Phys. Chem. Chem. Phys. **8**, 1985 (2006).

[34]T. Takatani, E. G. Hohenstein, M. Malagoli, M. S. Marshall, and C. D. Sherrill, J. Chem. Phys. **132**, 144104 (2010).

[35]C. D. Sherrill, T. Takatani, and E. G. Hohenstein, J. Phys. Chem. A **113**, 10146 (2009).

[36]D. C. Langreth, B. I. Lundqvist, S. D. Chakarova-Käck, V. R. Cooper, M. Dion, P. Hyldgaard, A. Kelkkanen, J. Kleis, L. Kong, S. Li, P. G. Moses, E. Murray, A. Puzder, H. Rydberg, E. Schröder, and T. Thonhauser, J. Phys.: Condens. Matter **21**, 084203 (2009).

[37]A. Puzder, M. Dion, and D. C. Langreth, J. Chem. Phys. **124**, 164105 (2006).

[38]J. Hooper, V. R. Cooper, T. Thonhauser, N. A. Romero, F. Zerilli, and D. C. Langreth, ChemPhysChem **9**, 891 (2008).